ISSN 1070-3284, Russian Journal of Coordination Chemistry, 2018, Vol. 44, No. 7, pp. 466–472. © Pleiades Publishing, Ltd., 2018.

Synthesis, Crystal Structure, and Electrochemical Properties of One Polyoxometalate-Based Silver(I) Compound with Keggin-Type $[PW_{12}O_{40}]^{3-}$ Anions[1]

H. X. Yang[a], W. J. Zhu[a], L. Y. Jin[a], Y. Bai[a, *], and D. B. Dang[a, **]

[a] *Henan Key Laboratory of Polyoxometalate Chemistry, Institute of Molecular and Crystal Engineering, College of Chemistry and Chemical Engineering, Henan University, Kaifeng, 475004 P.R. China*

**e-mail: baiyan@henu.edu.cn*

***e-mail: dangdb@henu.edu.cn*

Received September 15, 2017

Abstract—One polyoxometalate-based silver(I) compound $[Ag(2,2'\text{-Bipy})_2]_3(PW_{12}O_{40})$ (**I**) (2,2'-Bipy = 2,2'-bipyridine) has been synthesized and structurally characterized by IR spectroscopy, elemental analysis, XRPD and X-ray single-crystal structure analysis (CIF file CCDC no. 1572216). Compound **I** exhibits a crystalline three-dimentional supramolecular framework constructed by Ag-2,2'-Bipy coordination units and $[PW_{12}O_{40}]^{3-}$ template anions, in which there are multiform π···π interactions and hydrogen bonds. The cyclic voltammetric experiments show that compound **I** displays a good electrocatalytic activity toward the reduction of nitrite.

Keywords: polyoxometalate, silver(I) compound, crystal structure, electrochemical properties

DOI: 10.1134/S1070328418070035

INTRODUCTION

Polyoxometalates (POMs), a class of anionic early transition-metal oxide clusters, are of particular interest showing promise in many applications such as catalysis, nonlinear optics, medicine and materials science [1–5]. More importantly, POM anions are often recognized as the excellent inorganic building subunits to construct functional POM hybrids due to their designable structure, constituent elements and then special physical and chemical properties [6–8]. One of the fairly fundamental approaches is to introduce transition-metal complexes (TMCs) into POM hybrids and crystal engineering [9, 10]. This strategy is anticipated to obtain new POM-based compounds with a variety of structural motifs and interesting properties, which should flourish new functional materials. Among the numerous reports about POM-based compounds it was found that Keggin-type POMs are the most widely used POMs building subunits due to their easy preparation, high stability within a wide range of pHs, good solubility and thermal stability, and so on [11–13].

Ag(I), which has strong coordination ability, varieties of coordination modes and predominant optical properties, is often employed in the fields of design and synthesis of coordination compounds, as well as their applications [14–16]. For the past few years we have been interested in the synthesis of Ag(I)-containing POM-based crystalline species and have reported a series of products with N-donor ligands [17–21]. Continuing our studies on this respect, in this paper we report the synthesis and characterization of a Keggin-type POM-based compound $[Ag(2,2'\text{-Bipy})_2]_3(PW_{12}O_{40})$ (**I**) displaying an obvious electrocatalytic reduction performance for nitrite.

EXPERIMENTAL

All chemicals were of reagent grade quality obtained from commercial sources and used without further purification. $Na_9PW_9O_{34} \cdot 7H_2O$ was synthesized as described in the literature [22]. Elemental analyses (C, H, and N) were carried out on a Perkin-Elmer 240C analytical instrument. IR spectra were recorded with a Nicolet 170 SX FT-IR spectrophotometer in the region of 4000–400 cm^{-1} using KBr pellets. Powder X-ray diffraction patterns were recorded on a D/max-g A rotating anode X-ray diffractometer with a sealed Cu tube (λ = 1.54178 Å). The electrochemical measurement was carried out on a CHI 660E electrochemical workstation at ambient temperature. A conventional three-electrode system was used. The working electrode was a carbon paste electrode (CPE), with Pt wire as the counter elec-

[1] The article is published in the original.

Table 1. Crystallographic data and refinement parameters for compound **I**

Parameter	Value
Formula weight	4137.76
Temperature, K	296(2)
Crystal system	Monoclinic
Space group	*C*2/*c*
a, Å	10.6579(5)
b, Å	35.6869(16)
c, Å	21.6837(10)
β, deg	102.281(1)
V, Å^3	8058.6(6)
Z	4
ρ_{calcd}, g cm^{-3}	3.411
F(000)	7424
μ, mm^{-1}	17.876
θ Range for data collection, deg	1.9–25.0
Scan mode	ω
Number of collected reflections	20829
Number of unique reflections (R_{int})	7096 (0.042)
Number of reflections with $I > 2\sigma(I)$	5198
Number of parameters refined	598
GOOF (F^2)	1.03
R_1 (F)/wR_2 (F^2) ($I > 2\sigma(I)$)	0.0367/0.0780
R_1 (F)/wR_2 (F^2) (all data)	0.0574/0.0838
$\Delta\rho_{max}/\Delta\rho_{min}$, *e* Å^{-3}	1.20/−1.84

trode, and Ag/AgCl electrode was used as a reference electrode.

Synthesis of compound I. A solvent mixture (8 mL) of acetonitrile, water and DMSO (v : v : v = 2 : 1 : 1) was used as a buffer layer and very carefully layered onto 4 mL mixture of DMSO, water and HNO_3 (v : v : v = 1.5 : 1.5 : 1) of $AgNO_3$ (0.051 g, 0.30 mmol) and $Na_9PW_9O_{34} \cdot 7H_2O$ (0.15 g, 0.058 mmol) in a long and thin tube. Then, the solution of acetonitrile (3 mL) of 2,2'-Bipy (0.016 g, 0.10 mmol) was slowly layered onto the buffer layer. The solution was sealed and left for several days at ambient temperature. Yellow block crystals suitable for X-ray structure determination were isolated in the buffer layer in 36% yield based on 2,2'-Bipy.

For $C_{60}H_{48}N_{12}O_{40}PW_{12}Ag_3$ (*M* = 4137.76)

Anal. calcd., %	C, 17.40	H, 1.16	N, 4.06
Found, %	C, 17.32	H, 1.25	N, 3.97

IR (KBr; ν, cm^{-1}): 3436 w, 1627 w, 1590 m, 1472 m, 1437 m, 1315 w, 1234 w, 1177 w, 1155 w, 1080 s, 979 vs, 891 s, 819 vs, 806 vs, 759 m, 642 w, 619 w, 595 w, 522 m.

X-ray crystallography. A suitable crystal of size 0.25 × 0.22 × 0.17 mm was chosen for the crystallographic study and mounted on Bruker Smart APEX II CCD diffraction measurements were performed at room temperature using graphite-monochromatized MoK_α radiation (λ = 0.71073 Å). The structure was solved by direct methods and refined on F^2 by using full-matrix least-squares methods with the SHELXL-97 program package [23, 24]. Space group, lattice parameters and other relevant information are listed in Table 1, and selected bond lengths and angles are given in Table 2.

Supplementary material has been deposited with the Cambridge Crystallographic Data Centre (CCDC no. 1572216 (**I**); deposit@ccdc.cam.ac.uk or http://www.ccdc.cam.ac.uk).

RESULTS AND DISCUSSION

The IR spectrum of compound **I** gives clear evidences of the characteristic bands of α-Keggin-type $[PW_{12}O_{40}]^{3-}$ in the range of 1100–700 cm^{-1}. The strong peak at 1080 cm^{-1} is ascribed to the ν(P–O) stretching vibration. The absorption bands at 979 and 891 cm^{-1} should be attributed to ν(W = O_t) (terminal oxygen) and ν(W–O_b–W) (bridging oxygen), which are similar to those of α-$H_3[PW_{12}O_{40}]$ [25–27]. The bands which appear at 819 and 806 cm^{-1} show the stretching frequencies ν(W–O_c–W) (central oxygen). Those with variable intensity in the frequency range of 1627–1437 cm^{-1} correspond to ν(C=N) and ν(C=C) of 2,2'-Bipy groups, which agrees well with those of relevant compounds [28]. These results were finally confirmed by X-ray crystallography.

Single-crystal X-ray structural analysis revealed that compound **I** features a three-dimentional supramolecular framework in which Keggin-type polyanion clusters as ionic templates to balance the charge of Ag-2,2'-Bipy units. As shown in Fig. 1, the asymmetry unit consists of a half $[PW_{12}O_{40}]^{3-}$ polyanion, one and a half Ag-2,2'-Bipy coordination units. The polyoxoanion $[PW_{12}O_{40}]^{3-}$ is a typical α-Keggin structure. In $[PW_{12}O_{40}]^{3-}$, the P atom is located on a center of inversion, which is incompatible with the tetrahedral symmetry of the Keggin structure. Consequently, the polyoxoanion cluster was modelled as disordered over two orientations and the P atom is surrounded by a cube of eight O atoms, each with a site-occupancy factor of 0.5. The P–O distances range from 1.506(11) to 1.551(11) Å, and the OPO angles are in the range of 107.1(6)°–111.8(6)°. Each W atom exhibits a distorted WO_6 octahedral geometry. Twelve WO_6 octahedra are arrayed all around PO_4 polyhedron and linked into a

Table 2. Selected bond lengths (Å) and bond angles (deg) of **I***

Bond	*d*, Å	Bond	*d*, Å	Bond	*d*, Å
P(1)−O(20)	1.551(11)	P(1)−O(23)	1.506(11)	P(1)−O(21*A*)	1.506(10)
P(1)−O(21)	1.507(10)	P(1)−O(22)	1.523(12)	W(1)−O(1)	1.664(7)
W(1)−O(9)	1.879(7)	W(1)−O(8)	1.892(7)	W(1)−O(10)	1.898(8)
W(1)−O(11)	1.908(7)	W(1)−O(20)	2.429(11)	W(1)−O(21)	2.483(12)
W(2)−O(2)	1.662(9)	W(2)−O(11)	1.887(8)	W(2)−O(12)	1.868(8)
W(2)−O(21)	2.509(10)	W(3)−O(3)	1.663(6)	W(3)−O(14)	1.871(8)
W(3)−O(10)	1.884(8)	W(3)−O(13)	1.906(6)	W(3)−O(12)	1.908(7)
W(3)−O(21)	2.461(11)	W(3)−O(22)	2.479(11)	W(4)−O(4)	1.656(9)
W(4)−O(19*A*)	1.882(8)	W(4)−O(8*A*)	1.897(7)	W(4)−O(14)	1.909(6)
W(4)−O(15)	1.917(7)	W(4)−O(20*A*)	2.441(11)	W(4)−O(22)	2.494(13)
W(5)−O(5)	1.669(7)	W(5)−O(16)	1.862(8)	W(5)−O(15)	1.876(7)
W(5)−O(13)	1.888(6)	W(5)−O(17)	1.898(7)	W(5)−O(23)	2.429(11)
W(5)−O(22)	2.464(11)	W(6)−O(6)	1.654(9)	W(6)−O(18)	1.864(8)
W(6)−O(17)	1.886(8)	W(6)−O(23)	2.483(10)	W(7)−O(7)	1.682(6)
W(7)−O(19)	1.897(9)	W(7)−O(9)	1.901(7)	W(7)−O(16)	1.926(9)
W(7)−O(18)	1.927(8)	W(7)−O(20)	2.520(10)	Ag(1)−N(1)	2.287(8)
Ag(1)−N(2)	2.445(9)	Ag(1)−N(3)	2.297(8)	Ag(1)−N(4)	2.444(9)
Ag(2)−N(5)	2.254(8)	Ag(2)−N(6)	2.430(11)		
Angle	ω, deg	Angle	ω, deg	Angle	ω, deg
O(23*A*)P(1)O(23)	71.5(7)	O(23)P(1)O(22)	66.9(6)	O(23)P(1)O(21*A*)	177.0(7)
O(21)P(1)O(22)	70.2(6)	O(23)P(1)O(21)	107.7(5)	O(21*A*)P(1)O(21)	73.2(8)
O(23)P(1)O(22*A*)	111.8(6)	O(21)P(1)O(22*A*)	111.1(7)	O(22)P(1)O(22*A*)	178.5(9)
O(20)P(1)O(20*A*)	174.7(8)	O(23)P(1)O(20)	75.8(6)	O(21*A*)P(1)O(20)	107.2(6)
O(21)P(1)O(20)	68.3(6)	O(22)P(1)O(20)	110.2(6)	O(23)P(1)O(20*A*)	108.7(6)
O(21)P(1)O(20*A*)	107.1(6)	O(22)P(1)O(20*A*)	69.9(6)	O(1)W(1)O(8)	103.3(4)
O(1)W(1)O(9)	102.6(5)	O(1)W(1)O(10)	101.2(4)	O(9)W(1)O(8)	87.9(3)
O(1)W(1)O(11)	101.2(4)	O(1)W(1)O(20)	160.9(5)	O(8)W(1)O(10)	155.5(4)
O(8)W(1)O(11)	88.0(3)	O(8)W(1)O(20)	63.1(4)	O(9)W(1)O(10)	87.5(4)
O(9)W(1)O(11)	156.1(4)	O(9)W(1)O(20)	65.3(4)	O(10)W(1)O(11)	86.6(3)
O(11)W(1)O(20)	92.0(4)	O(1)W(1)O(21)	158.2(5)	O(9)W(1)O(21)	92.0(4)
O(8)W(1)O(21)	93.2(4)	O(10)W(1)O(20)	93.3(4)	O(10)W(1)O(21)	63.0(4)
O(11)W(1)O(21)	64.8(4)	O(20)W(1)O(21)	40.9(4)	O(2)W(2)O(12)	102.0(3)
O(12)W(2)O(11*A*)	88.2(4)	O(2)W(2)O(11)	101.3(2)	O(12*A*)W(2)O(12)	156.0(6)
O(12)W(2)O(11)	87.1(3)	O(11*A*)W(2)O(11)	157.4(5)	O(2)W(2)O(21)	159.0(2)
O(11)W(2)O(21)	64.5(4)	O(11)W(2)O(21*A*)	93.7(4)	O(12)W(2)O(21)	63.6(4)
O(21)W(2)O(21*A*)	41.9(5)	O(12)W(2)O(21*A*)	93.2(4)	O(3)W(3)O(14)	101.2(4)
O(3)W(3)O(10)	103.3(4)	O(3)W(3)O(22)	158.8(4)	O(10)W(3)O(22)	92.9(4)
O(14)W(3)O(10)	155.5(4)	O(3)W(3)O(13)	102.6(3)	O(14)W(3)O(13)	86.9(3)
O(10)W(3)O(13)	88.7(3)	O(3)W(3)O(12)	101.3(4)	O(14)W(3)O(12)	87.8(4)

Table 2. (Contd.)

Angle	ω, deg	Angle	ω, deg	Angle	ω, deg
O(10)W(3)O(12)	86.5(3)	O(13)W(3)O(12)	156.0(4)	O(3)W(3)O(21)	159.9(4)
O(14)W(3)O(21)	92.5(4)	O(10)W(3)O(21)	63.6(4)	O(13)W(3)O(21)	92.6(4)
O(12)W(3)O(21)	64.3(4)	O(21)W(3)O(22)	41.3(4)	O(14)W(3)O(22)	63.6(4)
O(12)W(3)O(22)	93.2(4)	O(13)W(3)O(22)	63.6(3)	O(4)W(4)O(8*A*)	103.0(4)
O(4)W(4)O(15)	101.6(4)	O(4)W(4)O(19*A*)	104.1(5)	O(4)W(4)O(20*A*)	161.4(4)
O(4)W(4)O(14)	101.0(5)	O(4)W(4)O(22)	156.7(4)	O(19*A*)W(4)O(14)	154.9(5)
O(8*A*)W(4)O(14)	87.4(3)	O(8*A*)W(4)O(22)	93.4(4)	O(19*A*)W(4)O(15)	88.1(4)
O(8*A*)W(4)O(15)	155.4(4)	O(14)W(4)O(15)	86.5(3)	O(14)W(4)O(22)	62.9(4)
O(19*A*)W(4)O(20*A*)	65.2(4)	O(8*A*)W(4)O(20*A*)	62.7(4)	O(14)W(4)O(20*A*)	90.7(4)
O(15)W(4)O(20*A*)	93.5(4)	O(20*A*)W(4)O(22)	41.8(4)	O(19*A*)W(4)O(22)	93.0(5)
O(15)W(4)O(22)	62.6(3)	O(5)W(5)O(16)	102.8(5)	O(5)W(5)O(15)	102.0(4)
O(17)W(5)O(22)	92.0(4)	O(23)W(5)O(22)	39.9(4)	O(5)W(5)O(23)	160.9(5)
O(16)W(5)O(15)	155.1(4)	O(5)W(5)O(13)	101.7(4)	O(16)W(5)O(13)	86.8(4)
O(15)W(5)O(13)	86.9(3)	O(5)W(5)O(17)	102.6(4)	O(16)W(5)O(17)	89.2(3)
O(15)W(5)O(17)	86.7(3)	O(13)W(5)O(17)	155.6(4)	O(13)W(5)O(22)	64.2(4)
O(16)W(5)O(23)	65.2(4)	O(15)W(5)O(23)	91.1(4)	O(13)W(5)O(23)	92.7(4)
O(17)W(5)O(23)	63.9(4)	O(5)W(5)O(22)	159.2(5)	O(16)W(5)O(22)	91.9(4)
O(15)W(5)O(22)	63.7(4)	O(6)W(6)O(18)	102.1(3)	O(18)W(6)O(18*A*)	155.7(6)
O(17)W(6)O(23*A*)	94.1(4)	O(23)W(6)O(23*A*)	41.5(5)	O(18)W(6)O(17*A*)	86.4(4)
O(6)W(6)O(17)	101.9(3)	O(18)W(6)O(17)	88.6(4)	O(17*A*)W(6)O(17)	156.3(5)
O(6)W(6)O(23)	159.2(2)	O(18)W(6)O(23)	65.4(4)	O(18)W(6)O(23*A*)	91.3(4)
O(17)W(6)O(23)	62.9(4)	O(7)W(7)O(9)	103.4(4)	O(7)W(7)O(19)	102.6(4)
O(7)W(7)O(16)	102.2(4)	O(7)W(7)O(18)	101.7(4)	O(7)W(7)O(20)	159.4(4)
O(19)W(7)O(9)	87.6(4)	O(9)W(7)O(20)	63.0(3)	O(19)W(7)O(16)	155.2(4)
O(9)W(7)O(16)	87.0(4)	O(16)W(7)O(20)	92.8(4)	O(19)W(7)O(18)	87.4(4)
O(9)W(7)O(18)	154.9(4)	O(16)W(7)O(18)	87.3(4)	O(18)W(7)O(20)	92.9(4)
O(19)W(7)O(20)	63.3(4)	W(2)O(11)W(1)	139.3(5)	W(2)O(12)W(3)	140.3(5)
W(1)O(8*A*)W(4)	139.6(6)	W(1)O(9)W(7)	139.6(5)	W(3)O(10)W(1)	140.6(5)
W(3)O(14)W(4)	141.3(4)	W(4)O(19*A*)W(7)	139.7(5)	W(5)O(13)W(3)	139.6(4)
W(5)O(16)W(7)	140.5(5)	W(5)O(15)W(4)	140.8(5)	W(6)O(17)W(5)	139.5(5)
W(6)O(18)W(7)	140.4(5)	N(1)Ag(1)N(2)	70.0(3)	N(1)Ag(1)N(3)	161.0(3)
N(1)Ag(1)N(4)	110.9(3)	N(3)Ag(1)N(4)	70.0(3)	N(3)Ag(1)N(2)	112.4(3)
N(4)Ag(1)N(2)	170.7(3)	N(5)Ag(2)N(6)	70.2(3)	N(5*B*)Ag(2)N(5)	129.3(4)
N(5*B*)Ag(2)N(6)	153.6(4)	N(6)Ag(2)N(6*B*)	98.8(6)		

* Symmetry codes: (*A*) $-x, y, 1/2 - z$; (*B*) $2 - x, y, 3/2 - z$; (*C*) $-1/2 + x, 1/2 - y, -1/2 + z$.

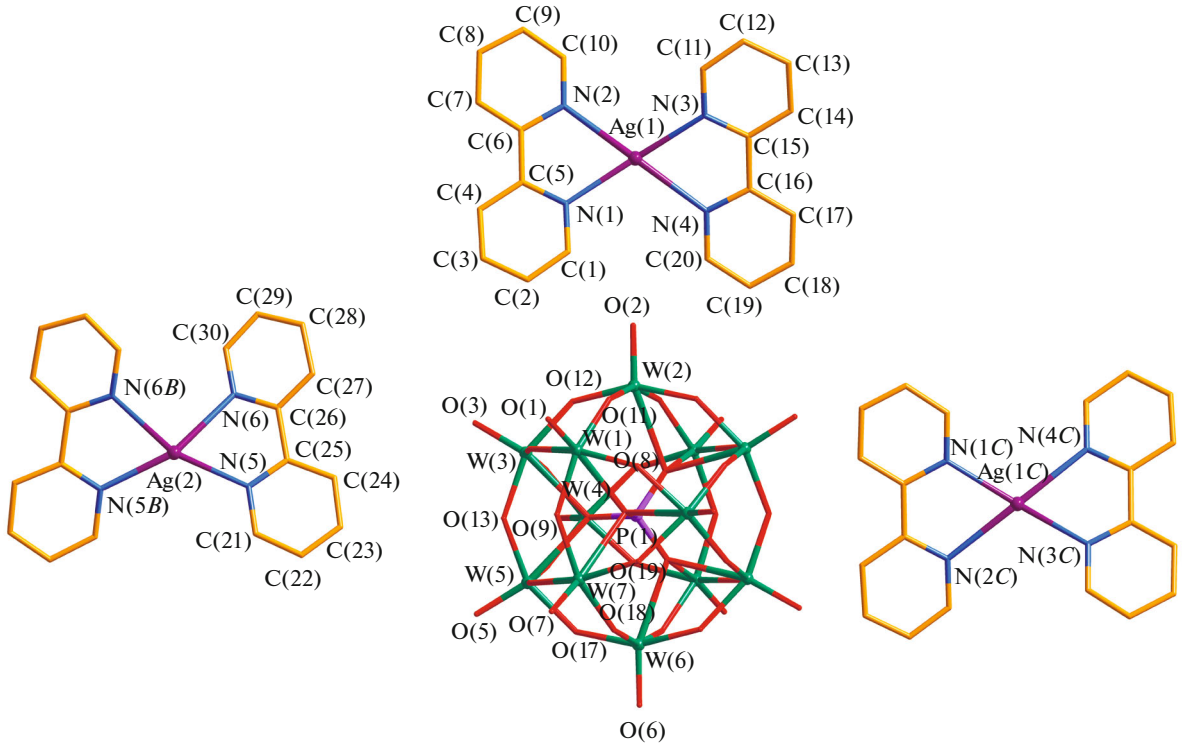

Fig. 1. The structure of compound **I** and the coordination environment of Ag(1) and Ag(2) centers (symmetry codes: (*B*) $2 - x$, y, $3/2 - z$; (*C*) $-1/2 + x$, $1/2 - y$, $-1/2 + z$).

polyanion $[PW_{12}O_{40}]^{3-}$ through corner– or edge–sharing. Three kinds of W–O_t, W–O_b and W–O_c distances are in the ranges of 1.654(9)–1.682(6), 1.862(8)–1.927(8), and 2.429(11)–2.509(10) Å, respectively.

Ag(1) and Ag(2) have similar coordinated environment with N_4 set from two 2,2'-Bipy ligands. The value of the geometric parameter τ for four-coordinate compounds is 0.20 for Ag(1) and 0.37 for Ag(2), indicates a distorted square planar geometry. The average Ag–N distance is 2.355 Å. Ag(2) lies in a special position of C_2 axis, consequently the two 2,2'-Bipy ligands are inter-related by Ag(2) atom.

In the solid state, it is interesting to note that there are three kinds of face-to-face π···π interactions involving pyridyl rings of adjacent 2,2'-Bipy (Fig. 2). The π···π interaction are found between the pyridyl ring N(1)C(1)–C(4) from the Ag(1)-2,2'-Bipy coordination unit and N(4)C(16)–C(20) from the adjacent Ag(1)-2,2'-Bipy unit with the shortest interplanar atom···atom separation of 3.37 Å, the centroid···centroid separation of 3.74 Å, and the dihedral angle of 5.5°, respectively. In addition, N(5)C(21)–C(25) ring from the Ag(2)-2,2'-Bipy coordination unit forms two types of π···π interactions with the two pyridyl rings N(1)C(1)–C(4) and N(3)C(11)–C(15) from two different adjacent Ag(1) units, respectively. The π···π interactions are characterized by the shortest interplanar atom···atom separation of 3.41 and 3.33 Å, the centroid···centroid separation of 3.95 and 3.80 Å, and the dihedral angle of 2.9° and 5.7°, respectively. Three kinds of C–H···O hydrogen bonds are found to stabilize the three-dimensional supramolecular network (Table 3). Apparently, the multiform interaction is favorable to obtain POM-based compounds with high rigidity (Fig. 3).

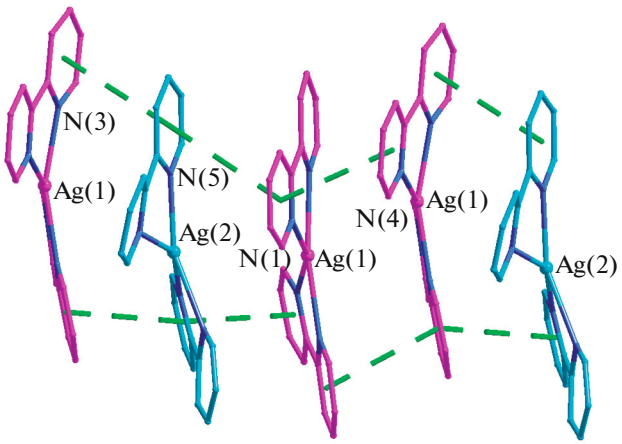

Fig. 2. The 1D chain of compound **I** showing π···π interactions with dashed lines.

Table 3. Geometric parameters of hydrogen bonds for compound **I**

D–H···A	Distance, Å			Angle DHA, deg	Symmetry codes of atom A
	D–H	H···A	D···A		
C(3)–H(3*A*)···O(3)	0.93	2.39	3.088(14)	132	$1/2 - x, 1/2 - y, 1 - z$
C(20)–H(20*A*)···O(2)	0.93	2.54	3.446(14)	166	
C(21)–H(21*A*)···O(6)	0.93	2.37	3.219(14)	153	$1 - x, -y, 1 - z$

To confirm the phase purity and to examine the crystallinity of bulk sample, the X-ray powder diffraction measurement was performed for compound **I**. The experimental XRPD pattern is in good agreement with that simulated based on the data of the single-crystal X-ray structure, indicating the good phase purity of the product.

The POM-modified CPE of compound **I** was used to reveal the electrochemical and electrocatalytic properties. The cyclic voltammetric behaviors in 1 M H_2SO_4 aqueous solution at different scan rates are presented in Fig. 4. In the potential range of +0.30 to –0.90 V, it can be clearly seen that there exit two pairs of reversible redox peaks **II–II′** and **III–III′** with the half-wave potentials $E_{1/2} = (E_{pc} + E_{pa})/2$ of –0.442 and –0.620 V (scan rate: 500 mV s^{-1}), respectively. Redox peaks **II–II′** corresponds to a one-electron process, while **III–III′** attributes to a two-electron process involving W centers of $[PW_{12}O_{40}]^{3-}$ [29–31]. With the increase of scan rates, the cathodic peak potentials of compound **I** shift to the negative direction and the corresponding anodic peak potentials shift toward the positive direction. There is also an irreversible anodic peak (**I**) with the potential at +0.149 V, which should be assigned to a one-electron oxidation process of the Ag centers [32]. The linear dependence of the cathodic peak currents on the scan rate confirms that the redox species are surface-controlled below the scan rate of 500 mV s^{-1} [33].

The cyclic voltammograms for electrocatalytic reduction of nitrite by compound **I** in 1 M H_2SO_4 aqueous solution can be seen from Fig. 5. In the potential range of +0.30 to –0.90 V, by increasing the concentration of nitrite, the reduction peak currents increased sharply, while the corresponding oxidation peak currents dramatically decreased, clearly indicating that compound **I** have a good electrocatalytic activity to the reduction of NO_2^- [34–36].

ACKNOWLEDGMENTS

This work was supported by the National Natural Science Foundation of China (nos. 21571049, 21471045), the Natural Science Foundation of Henan Province (nos. 162300410027, 162300410013), the

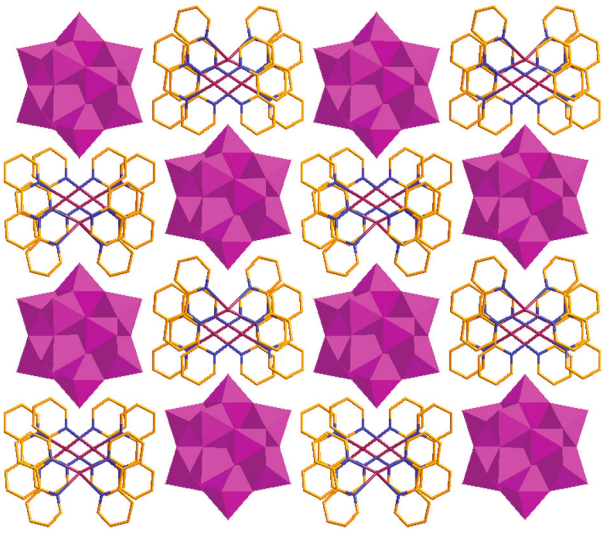

Fig. 3. The 3D supramolecular structure of compound **I**.

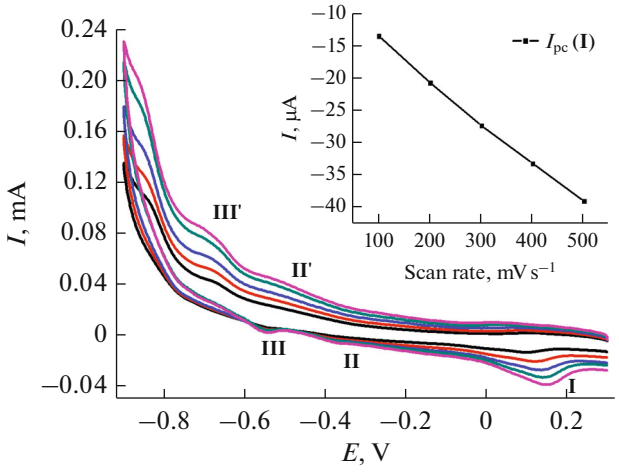

Fig. 4. The cyclic voltammograms for **I**-CPE in 1 M H_2SO_4 aqueous solution at different scan rates (from inner to outer: 100, 200, 300, 400, 500 mV s^{-1}) and the dependence of the cathodic peak current of wave (**I**) with different scan rates.

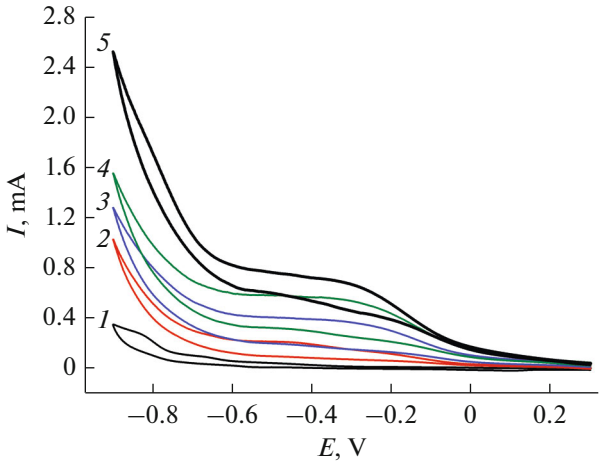

Fig. 5. The cyclic voltammograms of **I**-CPE in 1 M H_2SO_4 aqueous solution containing 0 (*1*), 20 (*2*), 40 (*3*), 60 (*4*), and 100 mM (*5*) $NaNO_2$ (scan rate: 100 mV s^{-1}).

Foundation of Henan Educational Committee (14A150022) and the Open Fund of Hubei Key Laboratory for Processing and Application of Catalytic Materials (no. 201721703).

REFERENCES

1. Wang, S.S. and Yang, G.Y., *Chem. Rev.*, 2015, vol. 115, p. 4893.
2. Nyman, M. and Burns, P.C., *Chem. Soc. Rev.*, 2012, vol. 41, p. 7354.
3. Zhang, Z.M., Zhang, T., Wang, C., et al., *J. Am. Chem. Soc.*, 2015, vol. 137, p. 3197.
4. Vanhaecht, S., Quanten, T., and Parac-Vogt, T.N., *Dalton Trans.*, 2017, vol. 46, p. 10215.
5. Zhang, Z., Zhao, J.W., and Yang, G.Y., *Eur. J. Inorg. Chem.*, 2017, p. 3244.
6. Sha, J.Q., Li, M.T., Yan, P.F., et al., *Dalton Trans.*, 2013, vol. 42, p. 7803.
7. Miras, H.N., Vilà-Nadal, L., and Cronin, L., *Chem. Soc. Rev.*, 2012, vol. 41, p. 7354.
8. Hou, Y.J., An, H.Y., Li, Y.Q., et al., *Dalton Trans.*, 2017, vol. 46, p. 8439.
9. Kikukawa, Y., Yamaguchi, K., and Mizuno, N., *Angew. Chem. Int. Ed.*, 2010, vol. 49, p. 6096.
10. Hu, T.P., Zhao, Y.Q., Jaglicic, Z., et al., *Inorg. Chem.*, 2015, vol. 54, p. 7415.
11. Mirzaei, M., Eshtiagh-Hosseini, H., Alipour, M., et al., *Coord. Chem. Rev.*, 2014, vol. 275, p. 1.
12. Sun, C.Y., Liu, S.X., Su, Z.M., et al., *J. Am. Chem. Soc.*, 2009, vol. 131, p. 1883.
13. Qin, J.S., Du, D.Y., Guan, W., et al., *J. Am. Chem. Soc.*, 2015, vol. 137, p. 7169.
14. Wu, H., Yang, J., Su, Z.M., et al., *J. Am. Chem. Soc.*, 2011, vol. 133, p. 11406.
15. Han, L.L., Zhang, X.Y., Sun, D.F., et al., *Cryst. Growth Des.*, 2014, vol. 14, p. 2230.
16. Yang, X.Y., Wei, T., Lan, Y.Q., et al., *Inorg. Chem.*, 2017, vol. 56, p. 8311.
17. Bai, Y., Zhang, G.Q., Dang, D.B., et al., *CrystEngComm*, 2001, vol. 13, p. 4181.
18. Dang, D.B., Zheng, Y.N., Bai, Y., et al., *Cryst. Growth Des.*, 2012, vol. 12, p. 3856.
19. Dang, D.B., An, B., Bai, Y., et al., *Dalton Trans.*, 2012, vol. 41, p. 13856.
20. Dang, D.B., Zheng, G.S., Bai, Y., et al., *Inorg. Chem.*, 2011, vol. 50, p. 7907.
21. Dang, D.B., Gao, H., Bai, Y., et al., *Inorg. Chem. Commun.*, 2010, vol. 13, p. 37.
22. Domaille, P.J., Hervea, G., and Teazea, A., *Inorg. Synth.*, 1990, vol. 27, p. 96.
23. Sheldrick, G.M., *Acta Crystallogr., Sect. A: Found. Crystallogr.*, 1990, vol. 46, p. 467.
24. Sheldrick, G.M., *Acta Crystallogr., Sect. A: Found. Crystallogr.*, 2008, vol. 64, p. 112.
25. Buru, C.T., Li, P., Mehdi, B.L., et al., *Chem. Mater.*, 2017, vol. 29, p. 5174.
26. Li, S.B., Ma, H.Y., Pang, H.J., et al., *Cryst. Growth Des.*, 2014, vol. 14, p. 4450.
27. Kong, Q.J., Hu, M.X., and Chen, Y.G., *J. Coord. Chem.*, 2011, vol. 64, p. 3237.
28. Lu, X.X., Luo, Y.H., Lu, C., et al., *J. Solid State Chem.*, 2015, vol. 232, p. 123.
29. Wang, X.L., Gao, Q., Tian, A.X., et al., *J. Solid State Chem.*, 2012, vol. 187, p. 219.
30. Tian, A.X., Lin, X.L., Ying, J., et al., *Dalton Trans.*, 2013, vol. 42, p. 9809.
31. Pope, M.T. and Varga, G.M., *Inorg. Chem.*, 1996, vol. 5, p. 1249.
32. Wang, S.H., Sun, Z.Y., Zhang, C.J., et al., *Inorg. Chem. Commun.*, 2014, vol. 41, p. 47.
33. Liu, D., Lu, Y., Tan, H.Q., et al., *Cryst. Growth Des.*, 2015, vol. 15, p. 103.
34. Tian, A.X., Ying, J., Peng, J., et al., *Cryst. Growth Des.*, 2010, vol. 10, p. 1104.
35. Liu, M.J., Zhang, P.P., Peng, J., et al., *Cryst. Growth Des.*, 2012, vol. 12, p. 1273.
36. Bi, L.H., Al-Kadamany, G., Chubarova, E.V., et al., *Cryst. Growth Des.*, 2009, vol. 48, p. 10068.